Progress In Electromagnetics Research Letters, Vol. 93, 89–97, 2020

Wideband Triple Resonance Patch Antenna for 5G Wi-Fi Spectrum

Arvind Kumar[1, *], Ayman Abdulhadi Althuwayb[2], and Mu'ath J. Al-Hasan[3]

Abstract—This study presents a triple resonance microstrip slotted antenna element for 5G (5.15–5.875 Wi-Fi band) applications. This antenna constitutes a rectangular patch stimulated with an I-shaped slot and two shorted metallic vias. This arrangement results in an enhancement of the bandwidth. The antenna features a wide impedance bandwidth (IBW) matching due to triple resonances when being properly excited by coax-probe feed. The IBW of the antenna ranges from 5–6 GHz band with three resonances at around 5.2, 5.5, and 5.8 GHz. Finally, the antenna is fabricated and measured, which displays a −10 dB IBW of 5.04–6.05 GHz (18.2%) featuring stable radiation and gain (around 7 dBi). Moreover, the measurements are in good agreement with simulations. On the account of the single-layered dielectric, this antenna can be easily mounted with active electronics.

1. INTRODUCTION

For the new generation of communication systems, microstrip patch/planar antennas have been commonly functional in various mobile technologies due to their obvious advantages, i.e., cost-effective manufacturing, light weight, low-profile configurations, and easy integration with active/passive electronic circuitry [1–7]. Additionally, 5G deployment is designed to provide fiber-like data rates, low latency, and high signal fidelity. To accomplish these performances, the antenna systems must be able to operate in a wide frequency range. Generally, most single-layered single-fed conventional microstrip patch antennas suffer from limited impedance bandwidth (IBW) due to their inherent characteristics of single resonance, typically 3–5% [3]. Hence, breakthroughs in antenna design are crucial for the global coverage of a wide frequency spectrum. Consequently, several advances have been addressed in the literature to improve the IBW of the microstrip patch antennas [8–16]. The most implemented way is to introduce slot(s) into the radiating patch(s), which can generate additional resonances in the vicinity of primary resonance and leads to bandwidth enhancement. This method helps to improve the bandwidth without introducing extra sizes; however, it affects radiation patterns at some degree. Another comprehensively used approach is loading parasitic strips/patches for electromagnetic coupling to the driven patch [8–10]. For example, a patch antenna with a gap-coupled sectoral patch is investigated in [8], which results in an IBW enhancement from 1.5 to 12.3%. In [9, 10], a stacked antenna structure is used for improving the IBW which helps to improve up to 20%. However, it increases not only cost but also physical size/design complexity. Moreover, embedding shorting vias into the dielectric slab is one of the prevailing techniques recommended in [11–19]. A printed triangle-shaped antenna with shorting vias and a V-slot is presented in [12]. It was concluded that slot and shorted-vias greatly affected the resistance and reactance of the antenna which improved the bandwidth matching conditions.

Furthermore, using similar techniques, the bandwidth enhancement mechanism was presented in [13–17, 19]. A triangular microstrip patch antenna with three gap coupled parasitic patches around

Received 16 July 2020, Accepted 15 September 2020, Scheduled 24 September 2020

* Corresponding author: Arvind Kumar (arvindkr.nitt@gmail.com).

[1] School of Electronics Engineering, Vellore Institute of Technology, Vellore, India. [2] Electrical Engineering Department, Jouf University, Sakaka, Aljouf 72388, Kingdom of Saudi Arabia. [3] Network and Communications Engineering Department, Al Ain University, Al Ain, United Arab Emirates.

the driven patch is presented. Three resonances can be obtained due to the introduction of the three parasitic patches which improve the operating frequency significantly.

In this work, a wideband microstrip patch antenna is presented for modern 5G Wi-Fi systems. The IBW of the antenna is enhanced by using an arrangement of rectangular patch loaded with an I-shaped slot, a couple of shorted vias, and coax probe feed. Finally, the antenna is fabricated and measured, which shows an IBW around 18% with stable radiation and gain performance with the simulated efficiency better than 95%.

2. ANTENNA CONFIGURATION AND DESIGN PROCESS

Figures 1(a), (b), and (c) show a perspective, top and lateral views of the proposed wideband antenna along with the coordinate system. The antenna structure has been designed by employing cost-efficient single-layered Rogers RT-Duroid-5880-DK-2.2 of thickness 1.57 mm. Design evolution of the proposed antenna is shown in Fig. 2. The design process of the antenna begins with a simple and widely used coaxial-fed conventional rectangular microstrip patch antenna. For the fundamental operating TM_{10} mode, ideally patch length L_p should be around $\lambda/2$, where λ is the wavelength in the medium filled with a dielectric of relative permittivity of ε_r. Here, λ is equal to $\lambda_o/\sqrt{\varepsilon_e}$, where λ_o is the free space wavelength, and ε_e is effective dielectric constant. Due to the fringing fields around the periphery of the patch, the value of ε_e is slightly less than ε_r. The width W_p of the patch has taken slightly more than $\lambda/2$, as it gives a better bandwidth without affecting radiation patterns. Initial dimensions of the patch are chosen for the centre frequency of 5.5 GHz. An I-shaped slot is etched on the rectangular patch. Basically, it reduces the capacitive reactance between the ground plane and patch, and facilitates additional resonance in the vicinity of the patch resonant frequency [20]. Furthermore, a couple of shorted vias are embedded which act as the inductive loading [20]. These vias produce their own resonant frequency, and their locations help in tuning the resonant frequencies in the desired 5G Wi-Fi spectrum. The IBW performances at the evolution stages are shown in Fig. 3. Characteristically, input impedance matching behavior of different stages of the design evolution is shown in Fig. 4. Hence, it is witnessed that the combination of the proposed slot and shorted vias leads to the enlargement of the bandwidth. Finally, IBW of this design ranges from 5.11 to 6.02 GHz with the triple resonant frequencies around the popular bands of 5.2, 5.5, and 5.8 GHz. The details of the optimized antenna parameters are listed in Table 1. In order to achieve the radiation in the broadside direction of the

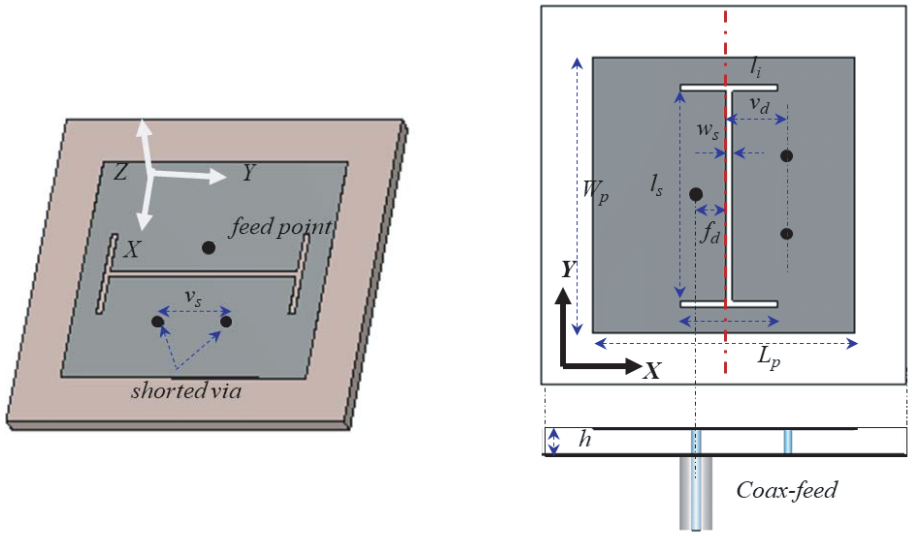

Figure 1. The structure of the proposed design concept: (a) The perspective view; (b) The top view and lateral view.

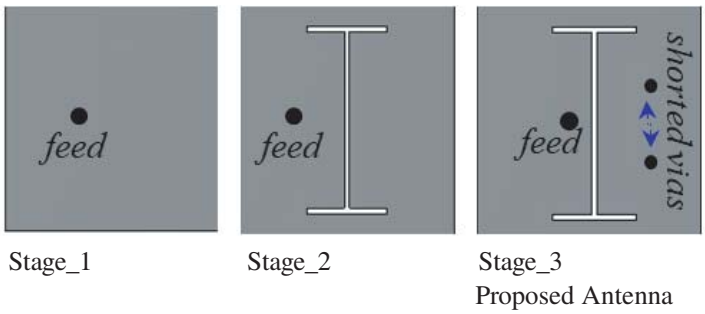

Figure 2. The stages of the design evolution.

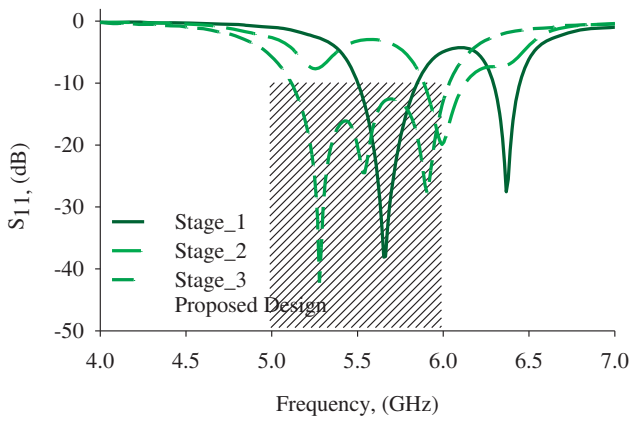

Figure 3. The responses of the design evolution stages.

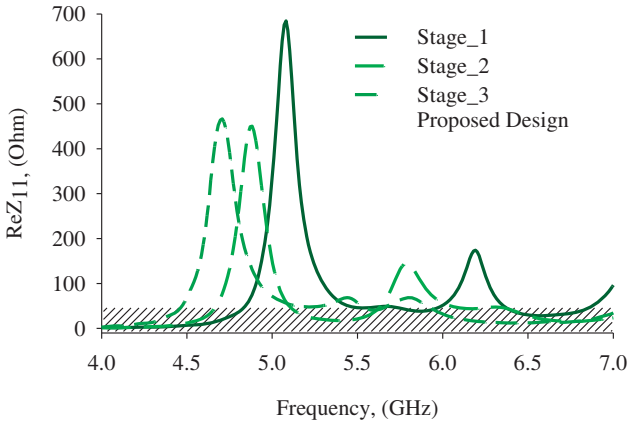

Figure 4. The input impedances of the antenna at the design evolution stages.

Table 1. The proposed antenna parameters and optimized values.

Parameters	W_p	L_p	l_s	w_s	v_d
Value (in mm)	34.6	33.05	26.4	0.8	8.12
Parameters	l_i	v_s	f_d	h	d
Value (in mm)	12.2	9.4	3.47	1.57	9.4

antenna, dimensions of the ground plane of the antenna are maintained larger than the width and length of the patch by four times of the dielectric thickness.

Moreover, the radiation performances of the antenna at the different resonant frequencies are illustrated with the help of corresponding current density (in A/m^2) [in Fig. 5]. For a better understanding of the operating bandwidth behavior of the antenna, an extensive parametric analysis of S-parameter is executed in Fig. 6. In each case, only a parameter under consideration is varied while all others are kept at optimal values, as listed in the aforementioned table. Overall, it can be concluded that the bandwidth performance of the antenna in the desired band is sufficiently stable. Fig. 6(a) shows that the impedance matching characteristics can be improved by changing the feed location along the x-axis. The antenna is designed at the centre frequency of 5.5 GHz, which predominantly depends on the length/width of the patch, and its parametric variations are shown in the Figs. 6(b), (c). The patch resonance can be merged with the slot resonance by making variations in the patch length/width. The parametric study of slot I-shaped slot dimensions is shown in Figs. 6(d), (e), (f), which essentially help to tune the bandwidth and resonant frequencies in the frequency band of interest. Furthermore, the parametric tuning of loaded vias is performed by varying offset distance of vias from centre of the patch

(Fig. 6(g)), and separation space between loaded vias (Fig. 6(h)) is studied. The resonant frequency and bandwidth can be tuned to maximise the operating bandwidth. The study in Fig. 6 presents tuning mechanism of the patch, slot, and loaded vias resonances.

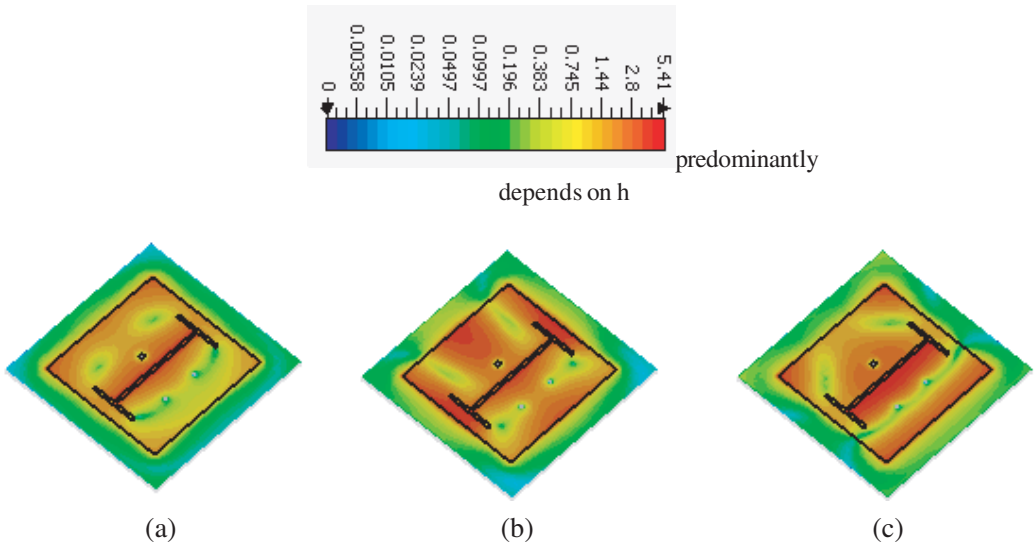

Figure 5. The current density at the resonant frequencies of: (a) 5.2; (b) 5.5 and (c) 5.9 GHz.

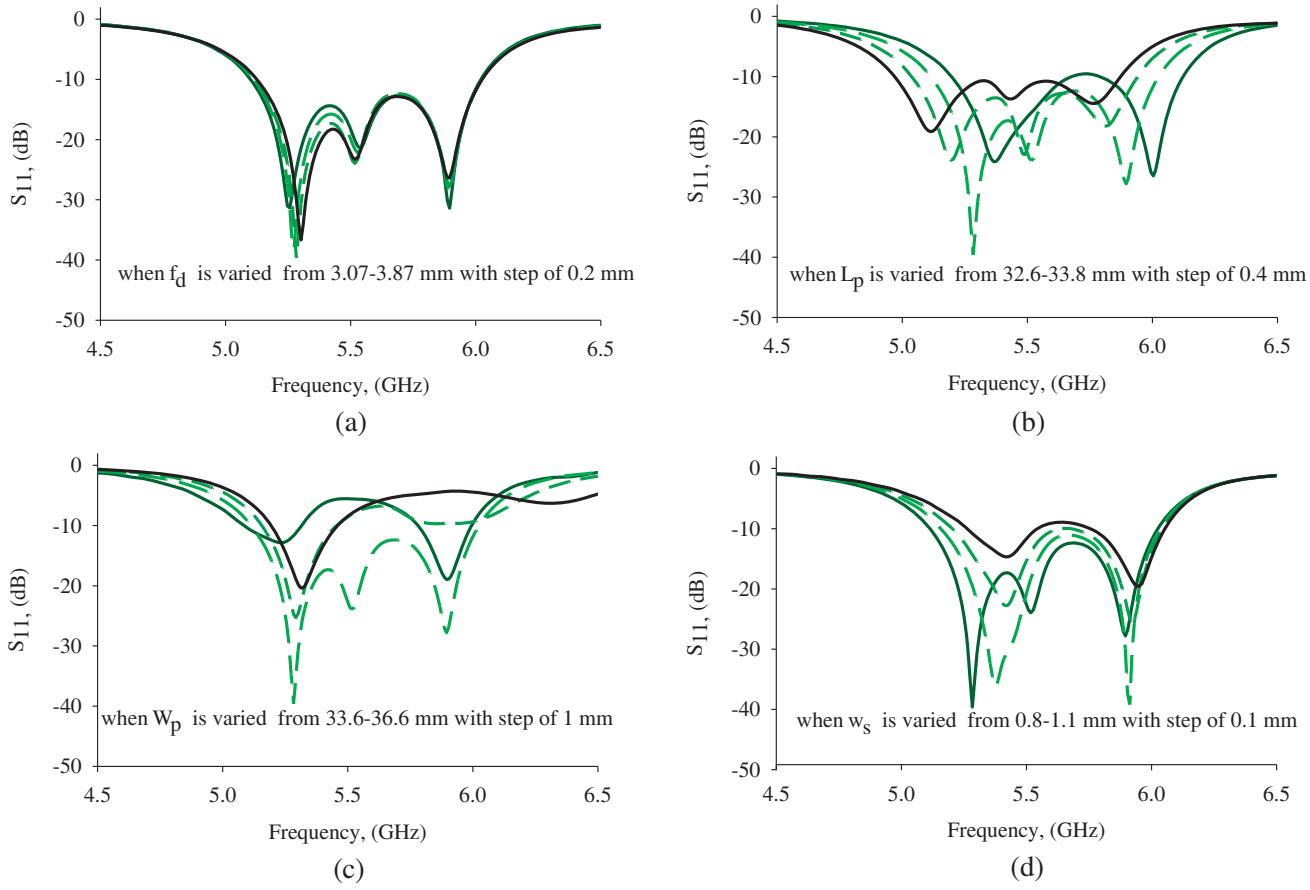

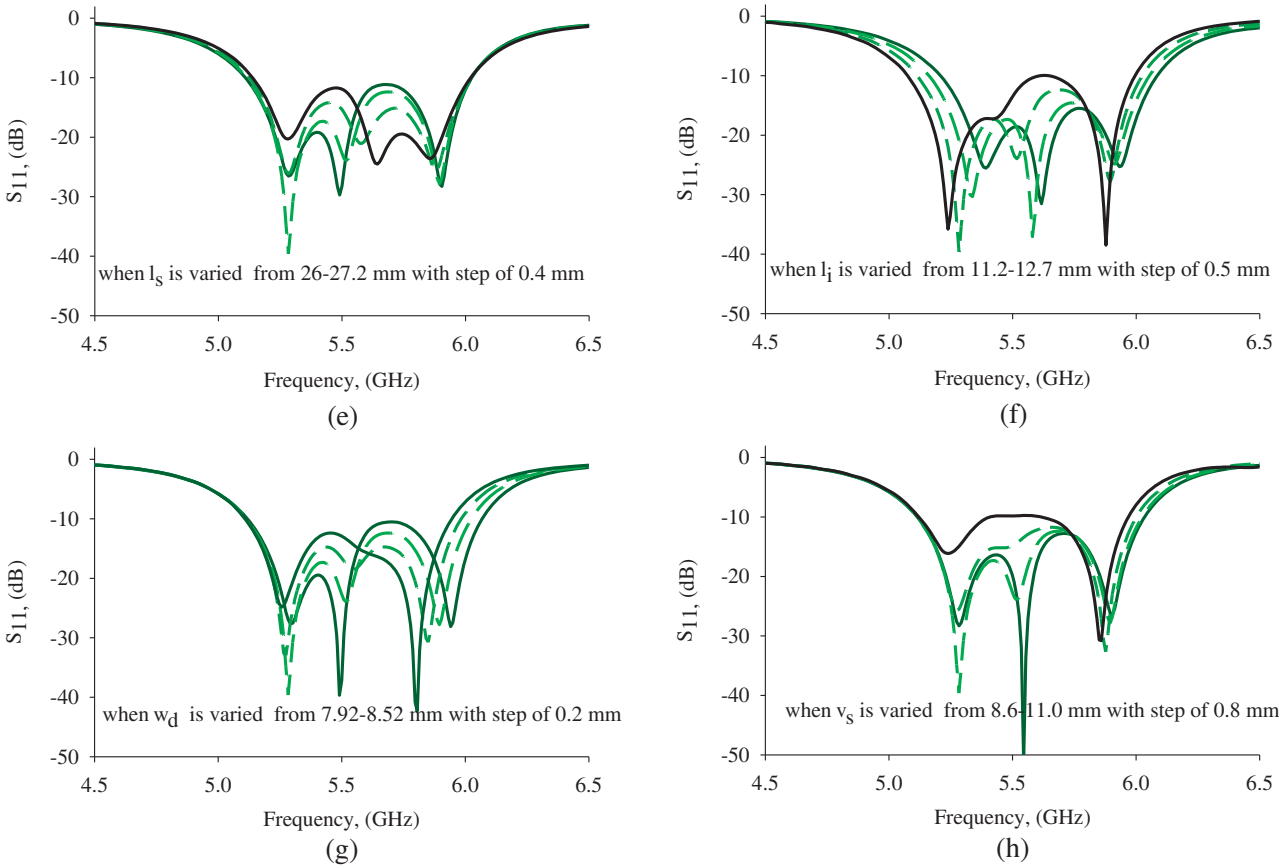

Figure 6. The S-parameters of the antenna with variation in: (a) f_d: feed offset from centre of the patch; (b) L_p: length of the patch; (c) W_p: width of the patch; (d) w_s: I-slot width; (e) l_s: length of the slot (medial); (f) l_i: length of the lateral edge of I-slot; (g) v_d: offset distance of vias from centre of the patch; (h) v_s: space between vias.

3. RESULTS AND DISCUSSIONS

In order to validate the predicted performance of the proposed concept, the design is fabricated, measured, and its snapshots are shown in Fig. 7. To realize low-footprint design, the thickness of the substrate is chosen as 1.57 mm as its IBW is sufficient for the recommended 5G Wi-Fi spectrum between 5.15 and 5.875 GHz. The manufacturing process of the antenna is performed with the help of

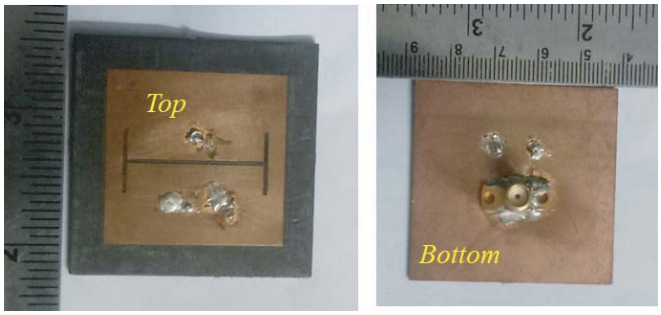

Figure 7. The top and bottom visuals of the fabricated antenna.

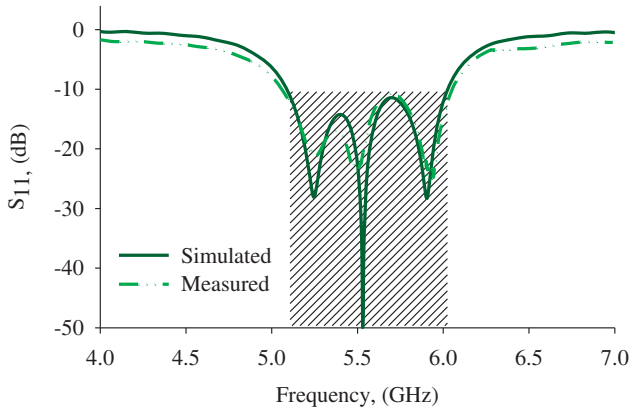

Figure 8. The simulated and measured reflection coefficients (S_{11}).

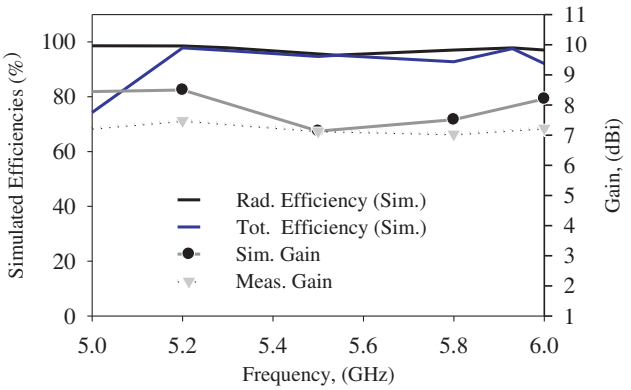

Figure 9. The antenna efficiencies and gain characteristics.

MITS Lab Eleven prototyping machine by using copper laminated dielectrics. The shorting metallic vias are implemented with copper rivets. The reflection coefficients $|S_{11}|$ of the antenna are measured with the help of Anritsu (*ShockLine MS46122B series*) vector network analyzers (VNA). Simulated and measured $|S_{11}|$ of the antenna are plotted in Fig. 8, and they show good agreement with each other.

The simulated $|S_{11}|$ parameter, below -10 dB ranges from 5.11 to 6.03 GHz (0.924 GHz), and the measured S_{11} (i.e., 5.04–6.05 GHz, 18.2% @ 5.5 GHz) almost overlaps the simulated counterpart. The operating frequency range of the antenna exhibits three resonant frequencies around 5.27, 5.49, and 5.93 GHz. This antenna shows uniform measured in-band gain performance, which is around 7 ± 0.5 dBi. The measured peak gains at the above mentioned resonant frequencies are typically about 7.2, 7.1, and 7.0 dBi, respectively. A comparative study of simulated and measured gains is shown in Fig. 9. The measured gains have fallen down by around 1.3 dBi. Moreover, simulated total antenna efficiency and radiation efficiency are shown in Fig. 9. As shown in the figure, these efficiencies are mostly ranging above 95% within the spectrum under consideration, which specifies the proposed design concept that the antenna has effectively radiated.

The far-field radiation pattern measurements are performed with the help of the test antenna in an anechoic chamber. Fig. 10 represents a study of the simulated and measured normalized radiation patterns at the resonant frequencies of 5.23, 5.54, and 5.93 GHz. It can be clearly observed that the measured and simulated co-polarization patterns are similar and in good agreement in boresight direction. Besides, the measured and simulated cross-polarization levels of the proposed antenna are also shown in Fig. 10. The measured cross-polarization levels are ranging from -16.4 to -29.4 dB across the operational spectrum. The measured front-to-back-ratios are around 9.2 to 33.3 dB across the operational spectrum. The detailed summary of the radiation patterns, including the 3-dB beamwidth in the vertical planes, is tabulated in Table 2. These results demonstrate that the antenna is essentially

Table 2. Summary of radiation performances of proposed Antenna at different resonant frequencies.

Electrical Parameters		Simulated Results			Measured Results		
Frequency (in GHz)		5.23	5.53	5.91	5.27	5.49	5.93
3-dB angular width (in degree)	At $\phi = 0°$	69.6	64.1	56.7	70.3	66.1	60.2
Cross polarization (in dB)		-34.8	-28.2	-35.6	-23.2	-21.6	-19.5
FTBR (in dB)		42.7	34.3	29.6	33.3	26.7	09.2
3-dB angular width (in degree)	At $\phi = 90°$	69.6	114.5	100.3	70.0	112.1	99.8
Cross polarization (in dB)		-37.5	-25.0	-26.5	-29.4	-24.4	-16.4
FTBR (in dB)		33.8	32.5	25.3	28.3	20.5	28.0

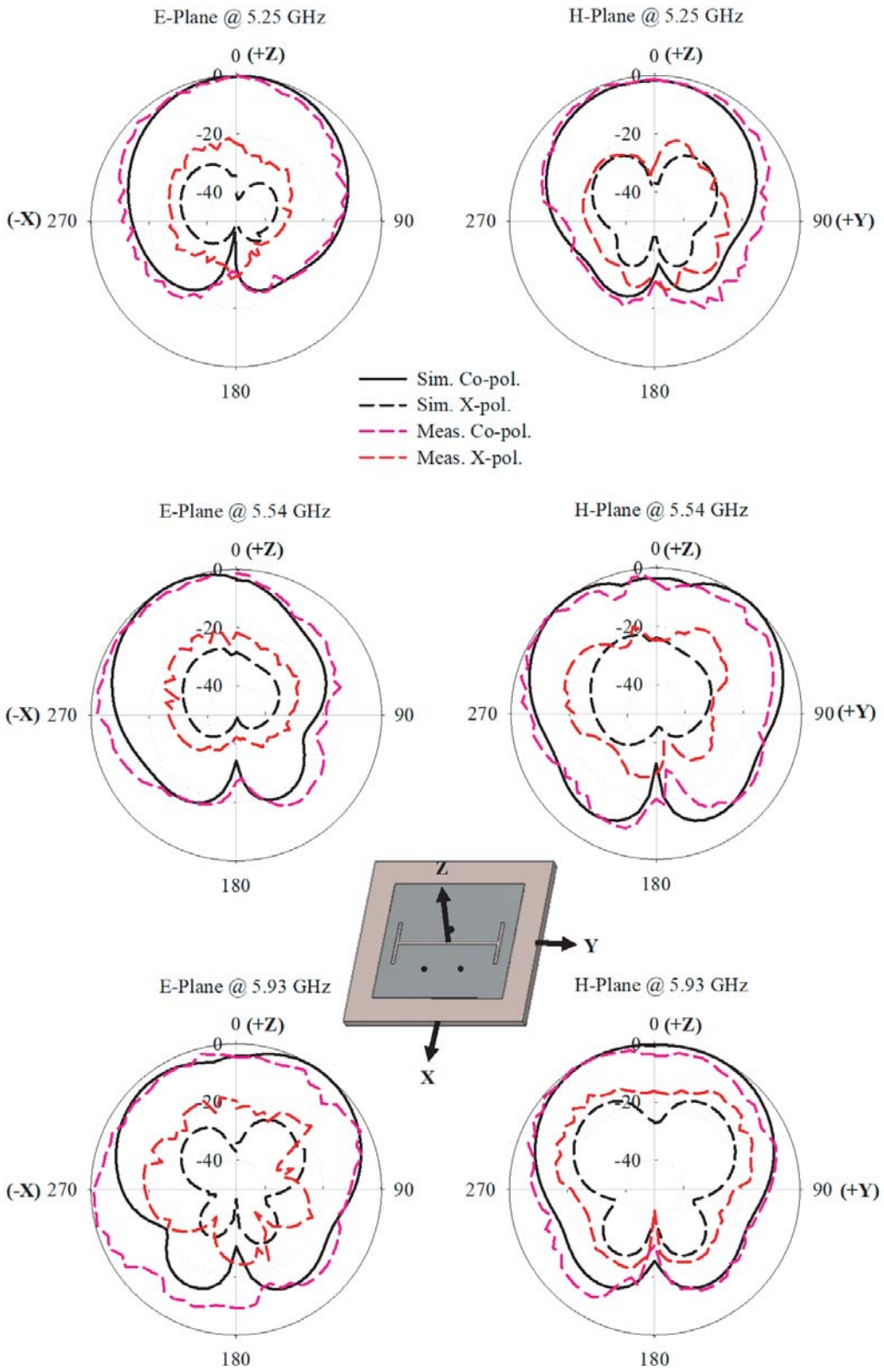

Figure 10. Simulated and measured normalized radiating profiles at 5.27, 5.49 and 5.93 GHz in E-plane and H-plane.

Table 3. Performance comparison of the proposed antenna with different type of bandwidth enhanced designs.

Ref.	Type of the antennas	Center Freq. (in GHz)	BW (in %)	Dielectric Constant	Peak Gain (dBi)	Gain Deviation (in dBi)	Cross-polar Level (in dB)	Efficiency (Peak)
Here,	Slot and via inspired microstrip patch antenna with probe feed	5.5	18.2	2.2	7.2	< 0.5	< -16.4	95%
[8]	Gap-Coupled Sectoral Patch Antenna	9.8	12.3	4.1	12	< 1	NA	95%
[10]	Strip-Slot Hybrid Multi-layered Structure	5.4	41	3.38, 3.38	10	< 4.5	< -19	NA
[21]	SIW cavity based octa-star slot with probe feed	10	16.35	2.2	5.3	< 0.65	< -20	95%
[22]	Aperture-Coupled Microstrip Antenna	2.5	15	21.96, 3.38	6.8	< 3	< -18	NA
[23]	HMSIW-based slotted antenna	5.3	13	2.2	7	< 2.3	< -10	85%

NA-Not Available

useful for 5G deployment of mobile communications. This design possesses a simple configuration and is very convenient to design and manufacture. To benchmark the performance of the proposed work against the previously reported bandwidth enhanced antennas, a comparative study is formulated in Table 3. It can be perceived that the proposed design owns a comparable performance with a low-profile and single layered structure. The radiation characteristics (gain deviation) of the proposed antenna are relatively more stable.

4. CONCLUSION

Here, a study of single-layered slotted rectangular patch antenna with a couple of loaded shorted vias is presented. Based on this configuration, a wide bandwidth with the same polarization is realized under triple-resonance mode. The antenna exhibits wide impedance bandwidth with stable radiation characteristics. The proposed antenna is suitable for 5G Wi-Fi communications, as the measured operating frequency is between 5.04 and 6.05 GHz. The antenna exhibits three resonant frequencies of 5.27, 5.49, and 5.93 GHz with peak gains of 7.2, 7.1, and 7.0 dBi, respectively. Moreover, the antenna is manufactured cost-efficiently with the help of the printed circuit board procedure and takes the advantages of practical implantation on a large ground plane.

ACKNOWLEDGMENT

This work is supported by the Abu-Dhabi Department of Education and Knowledge (ADEK) Award for Research Excellence 2019 under Grant AARE19-245.

REFERENCES

1. Huynh, T. and K. F. Lee, "Single-layer single-patch wideband microstrip antenna," *Electron. Lett.*, Vol. 31, No. 16, 1310–1312, Aug. 1995.

2. Kumar, A. and M. A. Al-Hasan, "A coplanar-waveguide-fed planar integrated cavity backed slotted antenna array using TE33 mode," *International Journal of RF and Microwave Computer-Aided Engineering*, e22344, Jun. 30, 2020.
3. Lee, K. F. and K. M. Luk, *Microstrip Patch Antennas*, Imperial College Press, London, England, 2011.
4. Kumar, A. and S. Raghavan, "Planar cavity-backed self-diplexing antenna using two-layered structure," *Progress In Electromagnetics Research Letters*, Vol. 76, 91–96, 2018.
5. Kumar, A., "Design of self-quadruplexing antenna using substrate-integrated waveguide technique," *Microwave and Optical Technology Letters*, Vol. 61, No. 12, 2687–9, Dec. 2019.
6. Divya, C., "SIW cavity-backed 24° inclined-slots antenna for ISM band application," *International Journal of RF and Microwave Computer-Aided Engineering*, Vol. 30, No. 5, e22160, May 2020.
7. Chaturvedi, D. and S. Raghavan, "SRR-loaded metamaterial-inspired electrically-small monopole antenna," *Progress In Electromagnetics Research C*, Vol. 81, 11–19, 2018.
8. Kandwal, A. and S. K. Khah, "A novel design of gap-coupled sectoral patch antenna," *IEEE Antennas Wirel. Propagat. Lett.*, Vol. 12, 674–677, 2013.
9. Rowe, W. S. T. and B. Waterhouse, "Investigation into the performance of proximity coupled stacked patches," *IEEE Trans. Antennas Propagat.*, Vol. 54, No. 6, 1693–1698, 2006.
10. Sun, W., Y. Li, Z. Zhang, and Z. Feng, "Broadband and low-profile microstrip antenna using strip-slot hybrid structure," *IEEE Antennas Wirel. Propagat. Lett.*, Vol. 16, 3118–3121, 2017.
11. Wong, H., K. K. So, and X. Gao, "Bandwidth enhancement of a monopolar patch antenna with V-haped slot for car-to-car and WLAN communications," *IEEE Trans. Vehicular Technol.*, Vol. 65, No. 3, 1130–1136, 2016.
12. Liu, J., Q. Xue, H. Wong, and H. W. Lai, "Design and analysis of a low-profile and broadband microstrip monopolar patch antenna," *IEEE Trans. Antennas Propagat.*, Vol. 61, No. 1, 11–18, 2013.
13. Liu, J. and Q. Xue, "Broadband long rectangular patch antenna with high gain and vertical polarization," *IEEE Trans. Antennas Propagat.*, Vol. 61, No. 2, 539–546, Feb. 2013.
14. Wang, J., Q. Liu, and L. Zhu, "Bandwidth enhancement of a differential-fed equilateral triangular patch antenna via loading of shorting posts," *IEEE Trans. Antennas Propagat.*, Vol. 65, No. 1, 36–43, 2017.
15. Wu, T. L., Y. M. Pan, P. F. Hu, and S. Y. Zheng, "Design of a low profile and compact omnidirectional filtering patch antenna," *IEEE Access*, Vol. 5, 1083–1089, 2017.
16. Shi, Y., J. Liu, and Y. Long, "Wideband triple- and quad-resonance substrate integrated waveguide cavity-backed slot antennas with shorting vias," *IEEE Trans. Antennas Propagat.*, Vol. 65, No. 11, 5768–5775, Nov. 1, 2017.
17. Liu, W., Z. N. Chen, and X. M. Qing, "Metamaterial-based low-profile broadband aperture coupled grid-slotted patch antenna," *IEEE Trans. Antennas Propag.*, Vol. 63, No. 7, 3325–3329, Jul. 2015.
18. Da Xu, K., H. Xu, Y. Liu, J. Li, and Q. H. Liu, "Microstrip patch antennas with multiple parasitic patches and shorting vias for bandwidth enhancement," *IEEE Access*, Vol. 6, 11624–11633, 2018.
19. Kumar, A. and S. Raghavan, "Bandwidth enhancement of substrate integrated waveguide cavity-backed bow-tie-complementary-ring-slot antenna using a shorted-via," *Defence Science Journal*, Vol. 68, No. 2, 197–202, Mar. 13, 2018.
20. Kumar, G. and K. P. Ray, *Broadband Microstrip Antennas*, Artech house, 2003.
21. Kumar, A., "Wideband circular cavity-backed slot antenna with conical radiation patterns," *Microwave and Optical Technology Letters*, Vol. 62, No. 6, 2390-7, Jun. 2020.
22. Liu, N. W., L. Zhu, W. W. Choi, and X. Zhang, "A low-profile aperture-coupled microstrip antenna with enhanced bandwidth under dual resonance," *IEEE Trans. Antennas Propagat.*, Vol. 65, No. 3, 1055–62, Jan. 24, 2017.
23. Chaturvedi, D. and S. Raghavan, "Wideband HMSIW-based slotted antenna for wireless fidelity application," *IET Microwaves, Antennas & Propagation*, Vol. 13, No. 2, 258–62, Jan. 9, 2019.